Source parameters of the 2011, Mw 5.2 Lorca earthquake (Spain)

J.A. López-Comino, F. Mancilla, J. Morales & D. Stich
Instituto Andaluz de Geofísica, Universidad de Granada, Granada, Spain
Departamento de Física Teórica y del Cosmos, Universidad de Granada, Granada, Spain

SUMMARY:
On May 11th 2011, an earthquake (M_W=5.2) hit the region of Murcia (Spain), shaking mainly to the town of Lorca and causing extensive personal and material damages. We estimate an oblique reverse faulting mechanism, a shallow hypocenter (4.6 km), at only 5.5 km epicentral distance from the Lorca center. Double difference relocations yield a rupture length of ~ 4 km, suggesting a propagation of the rupture from the northeast to the southwest along the Alhama de Murcia fault. We use the M_W 4.6 foreshock and an M_W 3.9 aftershock as empirical Green functions to estimate apparent source time functions, observing a clear directivity effect. We model apparent durations with a unilateral and asymmetric bilateral rupture, in both cases obtaining rupture directivity of ~N215°E, towards Lorca. Therefore, rupture directivity may have contributed to the unfavorable scenario caused by this terrible event.

Keywords: Lorca earthquake, Source parameters, directivity.

1. INTRODUCTION

On May 11th 2011, a magnitude M_W 5.2 earthquake hit the region of Murcia (Spain), shaking mainly the city of Lorca and causing extensive personal and material damages (~300 injured and 9 fatalities). Most municipal buildings were affected, presenting generally light to moderate damage. There was serious damage to historic buildings (churches, convents...) and even collapse of some houses. The Lorca earthquake, at 16:47 UTC (18:47 local time) was preceded by a M_W 4.6 foreshock at 15:05 UTC. There were also numerous aftershocks, the largest aftershock (M_W = 3.9) at 20:37 UTC on the same day. These events were located at distances of only 3 to 7 km from the town of Lorca at very shallow depths around 5 km. A maximum peak acceleration of 0.36 g was recorded in Lorca (*www.ign.es*). High damage caused by this earthquake of small magnitude close to a densely populated urban area (about 92,000 inhabitants) supports the need to study the seismic source parameters. In this way, we will complement and extend the seismological information has been obtained previously with point source models (location and moment tensor). So we can contribute to a description as exhaustive as possible of this earthquake.

The Lorca sequence was recorded at 22 broadband seismic stations within 250 km epicentral distance (Figure 1), mainly from the IAG and IGN permanent networks, as well as the temporary INDALO deployment by IAG. We use three-component displacement waveforms in least squares, time domain inversion for the deviatoric moment tensor for the fore-, main- and major aftershock (for technical details, see [Stich et al., 2003]). Waveforms are band-pass filtered between 20 and 50 s, and the closest stations are excluded from the inversion to avoid introducing near-field displacements. We test different source depths with 2 km increment, obtaining the lowest misfit at 4-6 km for the three main events. We obtain similar oblique reverse faulting mechanisms for the three events (Figure 1). Fault angle parameters are for the foreshock: strike N247°E, dip 46°, rake 40°; for the mainshock: N240°E, 54°, 44°; and for the aftershock N216°E, 63°, 22°. Moment magnitudes are 4.6 (M_0= 9.6×10^{15} Nm), 5.2 (M_0= 6.5×10^{16} Nm) and 3.9 (M_0= 7.3×10^{14} Nm), respectively.

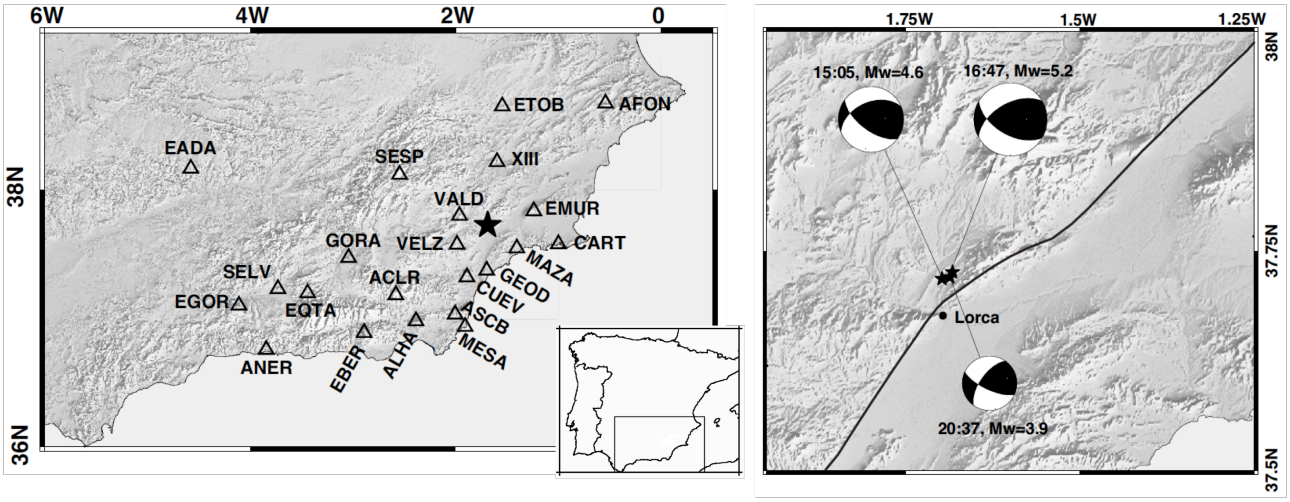

Figure 1. Left: Map of near-regional broadband stations used (triangles). Right: Surface trace of the Alhama de Murcia fault (AMF) in the epicentral area [Martínez-Díaz, 2002, Masana et al., 2004] and locations and moment tensor mechanisms for the Mw 5.2 Lorca earthquake, Mw 4.6 foreshock and Mw 3.9 aftershock (star) and regional broadband stations (triangles).

Taking into account local geology, we expect slip along the left-lateral, NW dipping nodal planes of our moment tensors, coincident with the strike and the kinematics of the Alhama de Murcia Fault (AMF) in this sector just north of Lorca (Lorca-Totana sector) where the fault trace shows a major bend (Figure 1). However, near real time locations of the aftershock sequence by IGN and IAG show a diffuse cloud of aftershocks, not allowing for the interpretation of any spatial or temporal trends. Consequently, it is necessary to perform hypocenter relocation. We used double-difference relocation of the entire sequence (113 events), using the HypoDD code (Waldhauser and Ellsworth, 2000, Waldhauser, 2001) (Figure 2). The location and strike of the epicenter distribution agrees well with the AMF NW of Lorca. If we associate the main concentration of early aftershocks with the fault surface that ruptured during the mainshock, we may estimate a rupture length of ~4 km. The mainshock hypocenter is situated near the NE end of the sequence, suggesting a scenario of rupture propagating predominately from NE to SW. We focus our attention on the directivity of rupture propagation. Directivity effects show up clearly in the azimuthal variation of apparent source durations and the spatial distribution of aftershocks. In this study, we address the characteristics of finite rupture through empirical Greens function analysis.

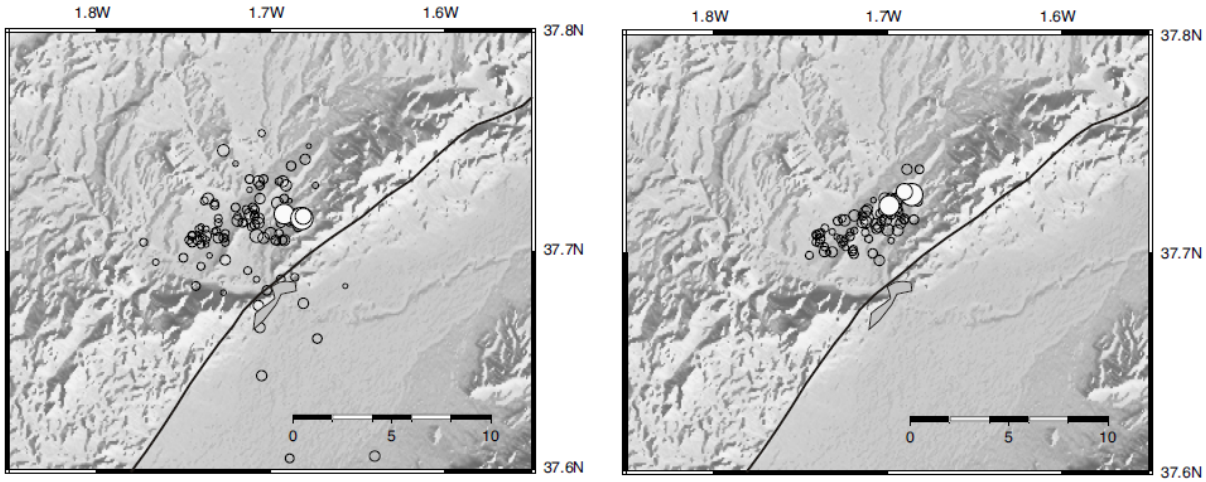

Figure 2. Left: Epicenters from single event locations including temporary stations. Right: Epicenters from double difference relocations. Circles with white fill are the three largest events of the sequence.

2. APPARENT SOURCE TIME FUNCTIONS & RUPTURE DIRECTIVITY.

The asymmetry of the aftershock distribution around the mainshock epicenter suggests asymmetry of rupture propagation. To corroborate this idea, we look into apparent source time functions (ASTFs) to confirm and quantify rupture directivity. We obtain ASTFs from empirical Green function deconvolution (Hartzell, 1978), using a Mw 4.6 foreshock and a Mw 3.9 aftershock with similar location and mechanism. We used two methods of deconvolution: spectral division and iterative time domain technique. Introducing a water level stabilizes spectral division. Water levels around 0.01 provide the most stable results, i.e. good signal to noise ratio and low back slip. Iterative time domain technique synthesizes the deconvolved function as a superposition of Gaussian pulses (Ligorría and Ammon, 1999; Kikuchi and Kanamori, 1982). We apply the deconvolution to P-wave windows (length equal to the S-P time) and S-wave windows (length 15-20s), and afterwards stack the ASTFs from the three components, resulting in one P- and one S-wave ASTF for each station (Figure 3 y 4).

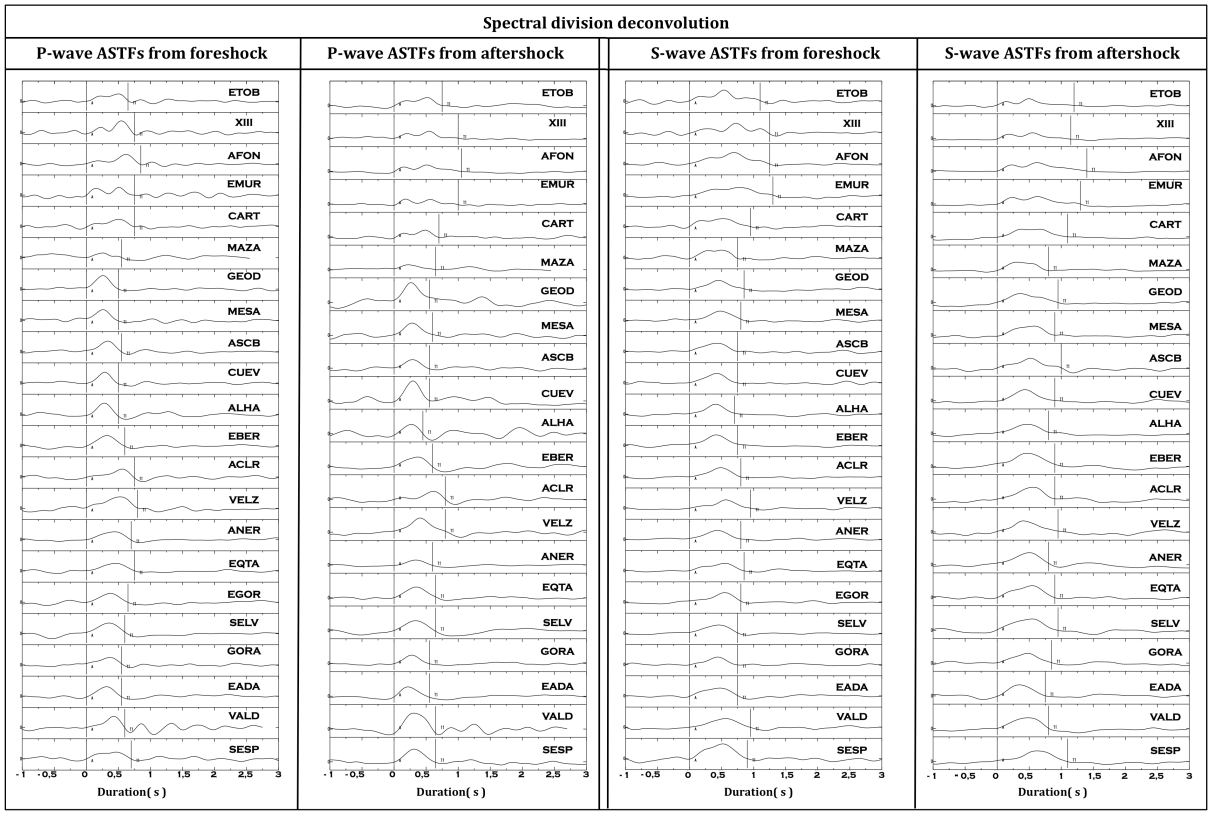

Figure 3. Apparent source time functions obtained from the spectral division deconvolution of foreshock and aftershock recordings, for P- and S-wave windows. ASTFs are sorted according to the azimuth. Manual pickings of onset and end of the moment rate functions are shown.

Both deconvolution methods have obtained consistent results, culminating in a single solution considering the apparent durations. We manually pick onset and end of our ASTFs, obtaining apparent source durations ranging from 0.45 to 1.05 s for P-waves and 0.7 to 1.4 s for S-waves. Picks are located at the intersection of the initial and final slopes of the ASTFs with the baseline, with uncertainties of about 0.05 s. Shape and duration of the ASTFs vary rather smoothly with station azimuth. A clear directivity effect shows up in the systematically longer durations towards NE and shorter durations towards SW (Figure 3 y 4). The wide ASTFs at NE azimuths show a succession of two or three pulses, indicating heterogeneous moment release along the rupture plane. In the narrow ASTFs at SW azimuths the three pulses merge into a less complex apparent time function. ASTFs from fore- and aftershock are similar in the case of S-waves, however this does not always hold for P-waves, where we observe a less clear azimuthal pattern using the foreshock. We conclude that, for the

short duration of P-wave ASTFs, the Mw 4.6 foreshock is apparently not a valid point source response.

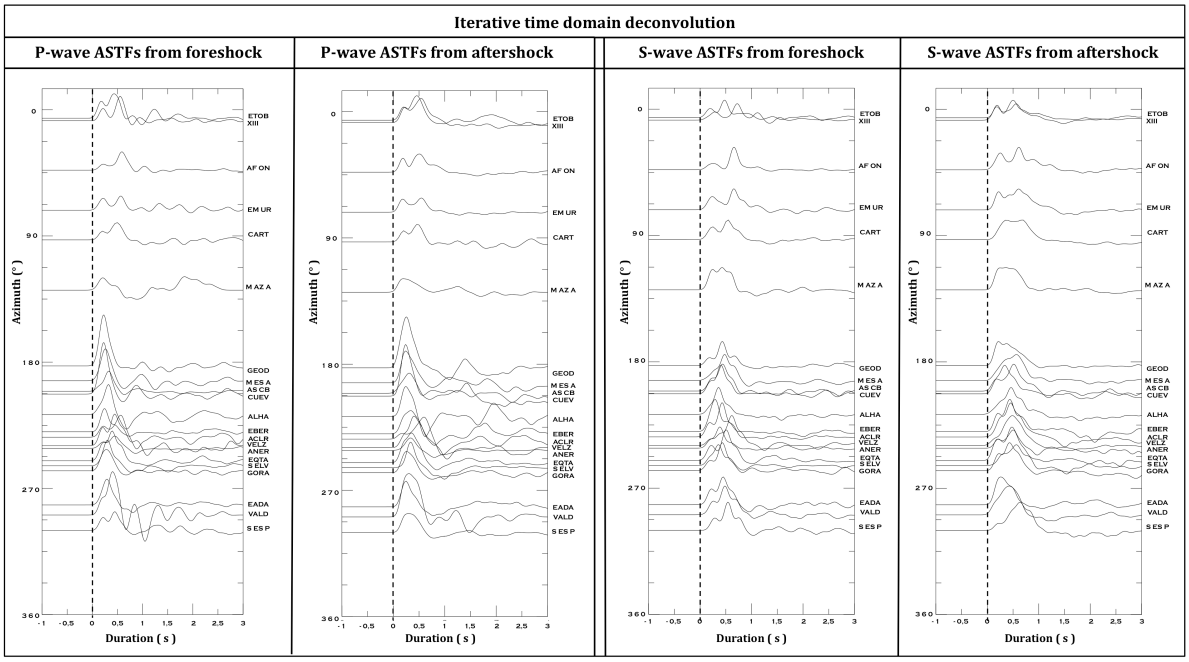

Figure 4. Apparent source time functions (apparent duration & azimuth) obtained from the iterative time domain technique of foreshock and aftershock recordings, for P- and S-wave windows.

We model apparent durations assuming a line source and adopting the parameterization by Cesca et al. 2011. We introduce a rise time of 0.4 s (compare Figure 3 y 4), and first investigate a pure unilateral rupture. To find duration, directivity and fault length, we apply a minimum search algorithm implemented in Matlab (lsqcurvefit command). This is a trust-region algorithm for multivarian non-linear functions based on the reflective Newton method (Coleman and Li, 1994, 1996). We achieve an adequate fit to observed apparent durations for rupture directivity towards ~N210°E (Figure 5a). Inferred rupture duration is 0.74 s from P- and 1.0 s from S-waves. This difference is an effect of the non-vertical dip of the fault plane; we have no direct observation of the undistorted source time function from a perspective perpendicular to the fault. The inferred rupture lengths for unilateral rupture are around 0.8 km. This is significantly less than the fault length expected from aftershock relocation, and would imply a very low rupture velocity of ~1km/s.

Modeling the more general case of an asymmetric bilateral line source, we achieve clearly better fits (Figure 5b). Inversion yields similar directivity (N209°E for S-waves and N231°E for P-waves) and, on average, a share of 70% of the rupture propagating towards SW and 30% towards NE. Rupture length and duration show larger variations due to some tradeoff, however the average rupture length of 2.4 km towards SW (that is, 3.4 km total rupture length) is consistent with the average duration (1.0 s, leading to a plausible rupture velocity of 2.4 km/s), and also consistent with the previous length estimate of 4 km corresponding to the main concentration of aftershocks.

3. DISCUSSION

The combination of moment tensor inversion, a relocation of the entire sequence, deconvolution of empirical Greens function and directivity analysis leads to a self-consistent description of the source characteristics for the 2011 Lorca earthquake. Our results support an identification of the 2011 earthquake with slip along the NE-SW trending AMF, specifically the so-called Lorca-Totana segment

[Martínez-Díaz, 2002, Masana et al., 2004], with similar orientation and kinematics as the NW-dipping, oblique left-lateral nodal plane of the moment tensor (Figure 1). The alignment of aftershocks and rupture directivity are close to NE-SW as well. Further support comes from the fact that the upper hemisphere projection of the rupture plane passes right through Lorca (Figure 5), located on top of the surface trace of the AMF.

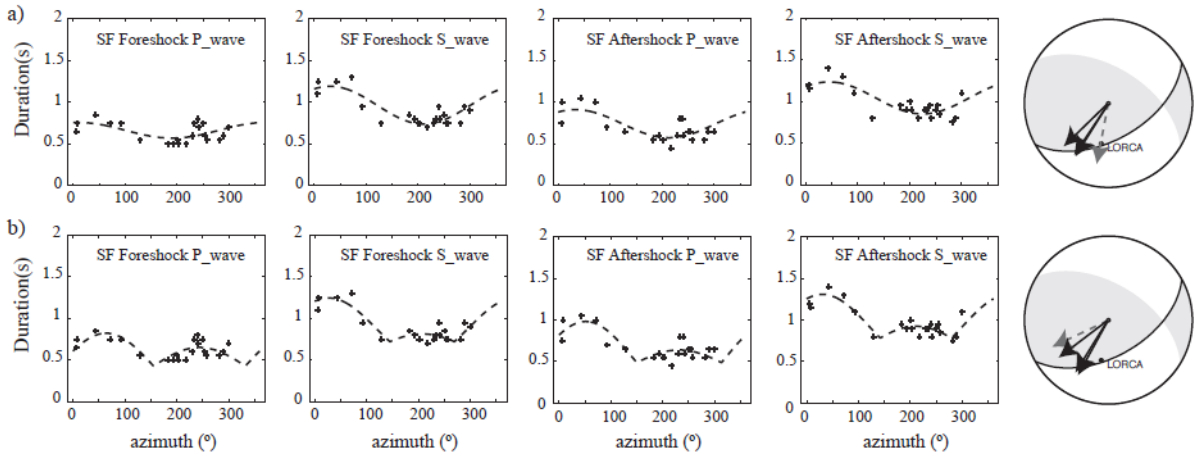

Figure 4. Plots of apparent source durations versus azimuth, and theoretical predictions for the best fitting horizontal line source, testing a) pure unilateral rupture (directivity of N190°E±44°, N211°E±20°, N213°E±31° and N225°E±29° for panels from left to right) and b) asymmetric bilateral rupture (directivity of N244°E±14°, N207°E±12°, N232°E±19° and N211°E±14°). Right panels: Upper hemisphere projections of the moment tensor fault plane, rupture directivity and the city center illustrate rupture propagation towards Lorca (N190°E).

The dense network of permanent and temporal seismic stations in the region provides good azimuthal coverage for the 2011 Lorca sequence. Despite the small size of the mainshock, we were able to recognize clear directivity effects. The apparent durations of source time functions obtained from S-waves vary by a factor of 2 (0.7-1.4s), with the longest ASTFs corresponding to stations at NE azimuths. The azimuthal pattern can be fit by an asymmetric bilateral rupture, with 70% of the rupture propagating in SW direction. The inferred rupture directivity of ~N220°E does not exactly match the N240°E strike of the fault plane, suggesting that there is an up-dip component of rupture propagation. The fault length inferred from directivity analysis (3.4 km) is close to our estimate from double-difference aftershock relocations (4 km). These are plausible values for an Mw 5.2 earthquake. From the definition of seismic moment [Aki and Richards, 2002], a rupture area of ~15 km^2 and a typical crustal rigidity of 30 GPa corresponds to ~0.14 m of average slip during the Lorca earthquake. Since subevents can be identified in several ASTFs (Figure 3 y 4), we may expect patches with larger than average slip along the rupture.

From our source analysis, we may think of several reasons why this relatively small earthquake had such a large impact. The outstanding factor is certainly the proximity to Lorca. Relocation places the earthquake at 4.6 km depth and 5.5 km epicentral distance from the city center. In addition, despite the low magnitude, a point source description is apparently not sufficient in this case, because the inferred rupture propagation up-dip and towards SW indicates the presence of significant slip even closer to Lorca (Figures 2 and 5). Probably the rupture stopped relatively close to the surface. Directivity towards Lorca (at N190°E from the epicenter) also leads to larger amplitudes and shorter duration of the source pulse (compare stations at similar azimuth in Figure 3 y 4, e.g. ASCB, CUEV), contribution to larger accelerations. Finally, Lorca is built almost on top of the fault trace and receives maximum S-wave radiation from any nearby quake on the AMF. We summarize that the location, radiation and rupture directivity combine to a very unfavorable scenario, as testified by a recorded horizontal peak acceleration of 0.36g.

AKCNOWLEDGEMENT
We are grateful to IGN, University of Alicante (AFON) and ROA/UCM/Geofon (CART) for providing high quality seismic data from their stations. We received financial support through Spanish National Projects CGL2008-01830 and TOPO-IBERIA (CSD2006-00041) and Junta de Andalucia Project P09-RNM-5100.

REFERENCES

Aki, K., P.G. Richards (2002), *Quantitative seismology* (2 ed.), University Science Books.

Coleman T., and Y. Li (1994), On the convergence of reflective Newton methods for large-scale nonlinear minimization subject to bounds, *Mathematical Programming*, 67, 189-224.

Coleman T., and Y. Li (1996), An interior, trust region approach for nonlinear minimization subject to bound, *SIAM Journal on Optimization*, 6, 418-445.

Cesca, S., S. Heimann, T. Dahm (2011), Rapid directivity detection by azimuthal amplitude spectra inversion, J. Seismol., 15, 147–164.

Hartzell, S.H. (1978), Earthquake aftershocks as Green's functions, *Geophys. Res. Lett*., 5, 1-4.

Kikuchi, M., and H. Kanamori (1982). Inversion of complex body waves, *Bull. Seism. Soe. Am.* 72, 491-506.

Ligorría, J. P., and C. J. Ammon (1999), Iterative deconvolution and receiver-function estimation, Bull. Seismol. Soc. Am., 89, 1395– 1400.

Martínez-Díaz, J. J. (2002). Stress field variety related to fault interaction in a reverse oblique-slip fault: the Alhama de Murcia Fault, Betic Cordillera, Spain, *Tectonophysics*, 356, 291-305.

Masana, E., J. J. Martínez-Díaz, J. L. Hernández-Enrile, and P. Santanach (2004), The Alhama de Murcia fault (SE Spain), a seismogenic fault in a diffuse plate boundary: Seismotectonic implications for the Ibero-Magrebian region, *J. Geophys. Res*., 109, B01301, doi:10.1029/2002JB002359

Stich, D., C. J. Ammon, and J. Morales (2003), Moment tensor solutions for small and moderate earthquakes in the Ibero-Maghreb region, *J. Geophys. Res*., 108, 2148, doi 10.1029/2002JB002057.

Waldhauser, F. and W.L. Ellsworth (2000), A double-difference earthquake location algorithm: Method and application to the northern Hayward fault, *Bull. Seism. Soc. Am.*, 90, 1353-1368.

Waldhauser, F. (2001), HypoDD: *A computer program to compute double-difference earthquake locations*, USGS Open File Rep., 01-113.